Morphology, Biodegradability, Mechanical, and Thermal Properties of Nanocomposite Films Based on PLA and Plasticized PLA

Guralp Ozkoc, Sebnem Kemaloglu

Department of Chemical Engineering, Kocaeli University, Kocaeli 41040, Turkey

Received 15 October 2008; accepted 13 May 2009
DOI 10.1002/app.30772
Published online 7 July 2009 in Wiley InterScience (www.interscience.wiley.com).

ABSTRACT: In this study, melt intercalation method is applied to prepare poly(lactic acid) (PLA) and poly(ethylene glycol) (PEG)-plasticized PLA nanocomposite films including 0, 3, and 5% organoclay (Cloisite 30B) using a laboratory scale compounder, which is connected to a microcast film device. To evaluate the nanomorphology and the dispersion state of the clays, X-ray diffraction (XRD) and transmission electron microscopy (TEM) are conducted. Tensile tests are performed to characterize the mechanical behavior of the films. Biodegradation rate is determined by degradation tests in composting medium. Differential scanning calorimeter (DSC) is applied to observe the thermal behavior of the films. XRD and TEM show that the exfoliation predominantly occurrs in plasticized PLA nanocomposites, whereas unexfoliated agglomerates together with exfoliated clays are observed in the nonplasticized PLA. Tensile tests indicate that the addition of 3% clay to the neat-PLA does not affect the strength; however, it enhances the modulus of the nanocomposites in comparison to neat-PLA. Incorporation of 3% clay to the plasticized PLA improves the modulus with respect to PLA/PEG; on the other hand, the strain at break value is lowered $\sim$ 40%. The increase in the rate of biodegradation in composting medium is found as in the order of PLA > PLA/PEG > 3% Clay/PLA/PEG > 5% Clay/PLA/PEG > 3% Clay/PLA. DSC analysis shows that the addition of 3% clay to the neat PLA results in an increase in T_g. The addition of 20% PEG as a plasticizer to the neat-PLA decreases T_g about 30°C, however incorporation of clays increases T_g by 4°C for the plasticized PLA. © 2009 Wiley Periodicals, Inc. J Appl Polym Sci 114: 2481–2487, 2009

Key words: poly(lactic acid); nanocomposite; biodegradation; packaging

INTRODUCTION

A great quantity of the plastic materials consumed in modernized countries is used for packaging purposes, which becomes a long-term solid waste problem. Compostable and biodegradable polymeric materials are therefore under great attention by both academy and industry. Poly(lactic acid) (PLA) is a linear, semicrystalline, aliphatic, biodegradable polyester that can be produced from lactic acid by the fermentation of renewable sources such as whey, corn, potato, or molasses. However, PLA is a relatively brittle material, thus it needs to be plasticized to produce flexible packaging films by cast film extrusion or blown film extrusion.[1] The potential plasticizers for PLA are citrate esters, poly(ethylene glycol), glucose monoesters, glycerol, oligomeric lactic acid.[1] These additives improve the flexibility and the processability of the PLA. However, it is more important to balance the stiffness and the flexibility of the packaging films. Organoclay-based nanocomposites can be a potential candidate because of their mechanical, thermal, gas barrier, and optical properties at low clay content.[2] PLA-based nanocomposites have been studied in recent years by applying melt intercalation technique. Ray et al.[3–7] investigated the effects of layered silicates on the properties of PLA. Results of their studies indicated that intercalation of the clays was achieved. The modulus of the nanocomposites improved and a significant reduction in oxygen permeability was observed. Pluta et al. studied the thermal and morphological properties of the PLA-based organoclay nanocomposites.[8] It was shown in their study that PLA and organoclays formed at least an intercalated structure. Thermal investigations showed an improvement in the nanocomposite thermal stability under oxidative conditions in comparison to those for unfilled PLA. The effects of plasticizer on the properties of PLA and PLA nanocomposites have also been studied. The addition of a plasticizer to the PLA usually reduces the glass transition temperature and the melting temperature.[9–11] It also decreases the modulus and the tensile strength, but it increases the elongation at break.[9,11] Most of the articles on PLA

Correspondence to: G. Ozkoc (guralp.ozkoc@kocaeli.edu.tr).

nanocomposites reports the properties of injection-molded specimens. To the best of our knowledge, there is a limited number of reports published on film blowing or film casting of PLA that are industrial processing methods to produce packaging films. In a study, plasticized PLA montmorillonite nanocomposites were compounded and blown-film processed.[12] The plasticizer and clay content were kept constant but the screw speed varied as the process parameter. It was reported that the nanocomposite films showed improvement in oxygen and water vapor barrier and Young Modulus in comparison to the neat PLA. It was also mentioned that the biodegradation rates changed with the addition of clay to the PLA.

The aim of this study is to examine the morphology, biodegradability, mechanical, and thermal properties of plasticized and nonplasticized PLA/organoclay (Cloisite 30B) nanocomposite cast films prepared by melt intercalation technique as an environmentally friendly packaging film. The plasticizer ratio was kept constant whereas the clay loading level varied as 0, 1, 3, and 5% by weight. A laboratory scale compounder connected to a melt film casting line was used as the processing tool to mimic the industrial cast film process.

EXPERIMENTAL

Materials

Poly(lactic acid) (PLA) was provided by Cargill-Dow at a number average molecular weight of 186,000. Cloisite® 30B, an organically modified montmorillonite (Southern Clay Products, USA), was used as the organoclay filler, because it was shown that Cloisite® 30B/PLA nanocomposites exhibited intercalated or partially exfoliated structures.[13–15] It was organically modified with methyl, tallow, bis-2-hydroxyethyl, quaternary ammonium by the supplier. The gallery spacing of this clay is reported as 1.85 nm. Poly(ethylene glycol) (PEG, MW = 1000 g/mol) (Sigma-Aldrich) was used as the plasticizer.

Compounding and film casting

PLA was dried for 12 h at 65°C, PEG and clay for 12 h at 35°C under vacuum before processing. PEG content was kept constant at 20% by weight in all compositions. Clay content was 0, 1, 3, and 5% by weight with respect to the matrix (PLA or PLA/PEG). The compounds were prepared in a corotating twin screw laboratory scale compounder (15 mL Microcompounder, DSM Xplore). This laboratory scale device can be either operated in continuous mode or in batch mode. To produce films, a cast film line (Micro film device, DSM Xplore) was connected to the laboratory scale compounder (see Fig. 1). The barrel temperature was 220°C, the screw speed was 100 rpm, and the residence time was 5 min under nitrogen atmosphere in compounding step. At the end of compounding, the compounder was shifted to force controlled mode from speed controlled mode to maintain a constant rate of throughput. A slit die with a thickness of 0.3 mm was used. To prevent necking and to fix the width, the film was cooled at the exit of the die by using an air-knife. The speed of collecting roller (speed controlled roller in Fig. 1) was arranged to obtain an average thickness of 0.25 ± 0.02 mm and width of 25 ± 2 mm film.

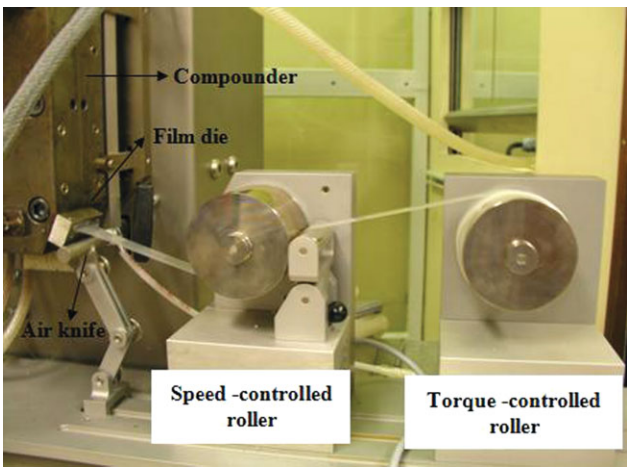

Figure 1 Cast film device connected to the laboratory scale compounder. [Color figure can be viewed in the online issue, which is available at www.interscience.wiley.com.]

Characterization

X-ray diffraction (XRD) analysis was conducted on nanocomposite films by using a RIGAKU D/MAX 2200/PC XRD using X-ray source of Cu Kα (λ = 1.54 Å) radiation generated at a voltage of 40 kV and current of 40 mA. The diffraction angle 2Θ was scanned from 0.5° to 10° at a scanning rate of 0.5°/min. Organoclay was analyzed in powder form under same conditions.

The nanomorphology of the films was examined by transmission electron microscope (TEM) (Philips CM200 TEM) at an acceleration voltage of 120 kV. Ultrathin sections of 70 nm in thickness were cryogenically cut with a diamond knife at a temperature of −100°C. All samples were trimmed parallel to the film casting direction.

Differential scanning calorimeter (DSC) analysis was performed using a Metler Toledo DSC 1 Star System between 0 and 200°C at a heating rate of 10°C/min under nitrogen atmosphere. Glass transition temperature, crystallization temperature, melting temperature, and corresponding enthalpies of

the films were obtained from DSC thermograms. Three replications were done from each batch in order to obtain an average value.

Tensile tests were performed according to ASTM D 882 using an Instron Universal Testing Machine. The crosshead speed was 10 mm/min. Five samples were tested from each batch. The average values were reported with the standard deviation.

To obtain biodegradation rate, 2-month-old compost was used as the degrading medium. The compost was kindly supplied from Mupa Mantar Tarım ve Gıda San. A.Ş., Kocaeli. It was a mixture of vegetable wastes, straw, and horse manure. The moisture content of the compost was determined as 70% by weight. This moisture level was maintained constant during biodegradation tests. The weight ratio of the films to the compost is 0.3% on dry basis. The films were buried into the compost and kept there at 30°C in a dark room. The change of weight of the dried films was measured every 10 days. The % weight loss was calculated with respect to initial dry-weight of the films.

To calculate water absorption (A), the method described in ASTM standard D570-98 was applied. The films were dried in an oven at 50°C for 24 h. Subsequently, they were weighed and immersed in distilled water at 25°C for 26 h. The films were taken out, and the surface moisture was wiped off with a paper tissue, and then weighed again. After the film was taken out from water, the container was placed in an oven for 24 h at 50°C to evaporate the water. The residuals were the water-soluble contents. The weight-gain of the films and the weight of the water-soluble residuals were counted as the total absorbed water. Water absorption (A) was calculated by eq. (1):

$$A = \frac{(W_1 - W_0 + W_2)}{W_0} \times 100 \quad (1)$$

where W_0 and W_1 are the weights of the films before and after being submerged in water, respectively, and W_2 is the weight of the water-soluble residual.

RESULTS AND DISCUSSION

Nanomorphology by TEM and XRD

XRD patterns of Cloisite 30B, 3% Clay/PLA, and 3% Clay/PLA/PEG nanocomposites are given in Figure 2. Cloisite 30B has a typical peak around $2\Theta \approx 5^\circ$ which corresponds to a basal spacing of 1.8 nm, which is consistent with the value of 1.85 nm reported by the manufacturer. When clays are compounded with PLA, the resulting pattern shows only two weak peaks around $2\Theta \approx 2^\circ$ and $2\Theta \approx 5^\circ$ that corresponds to the d-spacing of 4.4 and 1.8 nm, respectively. This indicates that most of the clays are

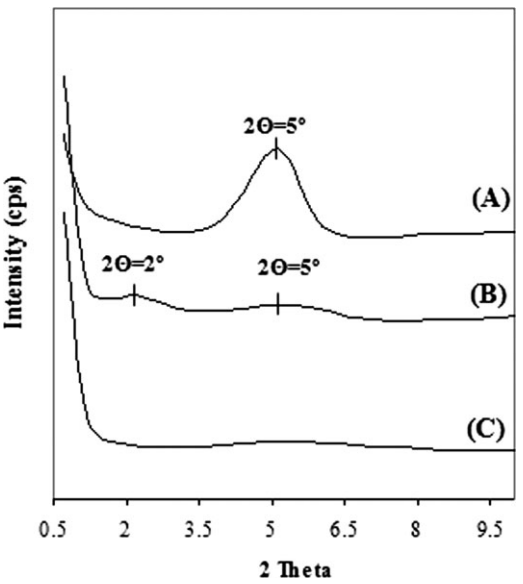

Figure 2 XRD patterns of (A) Clay (Cloisite®30B), (B) 3% Clay/PLA, and (C) 3% Clay/PLA/PEG nanocomposites.

intercalated or partially exfoliated by the help of shear forces during processing and diffusion of polymer chains through the clay galleries, but there still exist some unexfoliated clay agglomerates. The XRD pattern of plasticized PLA-based nanocomposites does not show a peak indicating more or less an exfoliated structure. For PEG as the plasticizer, it can be much easier to diffuse through clay galleries in comparison to PLA chains due to lower molecular weight; therefore, this may promote the exfoliation of the clays.

TEM micrographs of PLA-based nanocomposites are shown in Figure 3(A–C). The partially exfoliated clay layers are visible together with unexfoliated tactoids, which is consistent with the XRD patterns. The TEM micrographs of the nanocomposites based on PLA/PEG blends is given in Figure 4(A–C). It is observed that the clays are dispersed as submicron aggregates of several platelets stacked on top of each other. These aggregates seem to be 100–400nm in length and between 5 and 50 nm in thickness. When compared to the PLA-based nanocomposites, the level of dispersion of clay particles is improved by the addition of PEG as a plasticizer. The flow direction of the melt during film casting is shown with an arrow on the micrographs of both PLA- and PLA/PEG-based nanocomposites [see Figs. 3(A) and 4(A)]. It is seen that the clay layers are well oriented in the direction of the flow.

Differential scanning calorimeter

DSC thermograms of PLA, plasticized PLA, and their nanocomposites are shown in Figure 5 and thermal properties such as glass transition

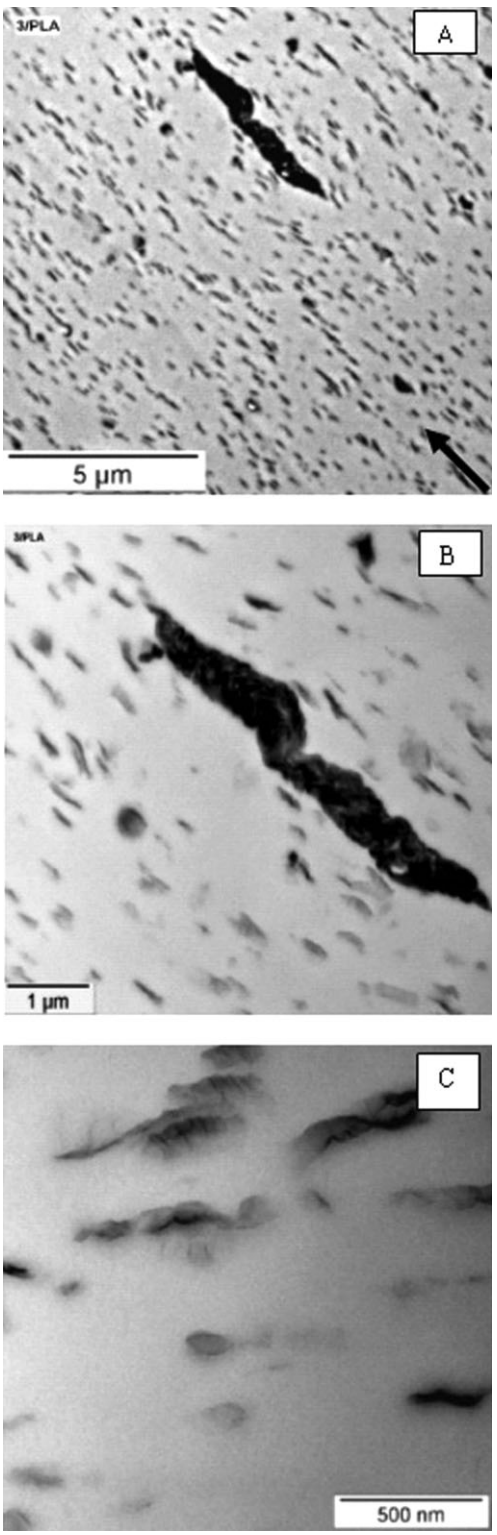

Figure 3 TEM micrographs of 3% Clay/PLA nanocomposite system at various magnifications.

temperature (T_g), cold crystallization temperature (T_c), melting temperature (T_m), melting enthalpy (ΔH_m), and degree of crystallinity (χ_c) are summarized in Table I. χ_c is calculated based on the enthalpy of fusion of 100% crystalline PLA, which is 93 kJ/g.[16]

The neat PLA is characterized by a T_g at 59.9°C, a cold crystallization peak at 106.1°C, and finally a melting peak at 152.6°C. The addition of 3% clay to

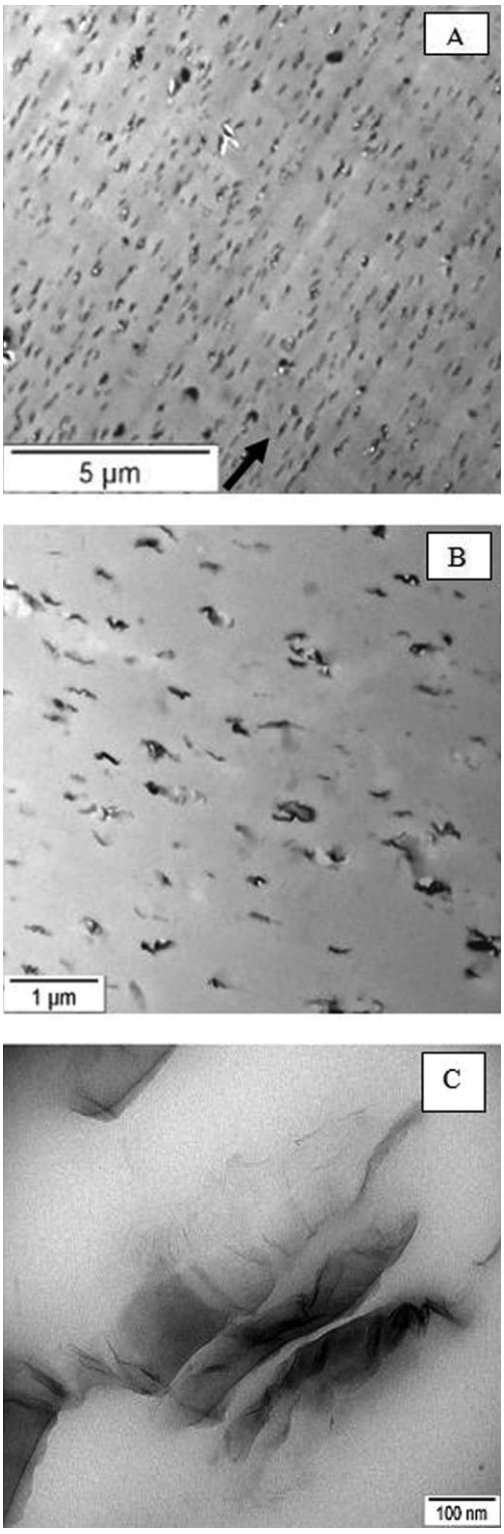

Figure 4 TEM micrographs of 3% Clay/PLA/PEG nanocomposite system at various magnifications.

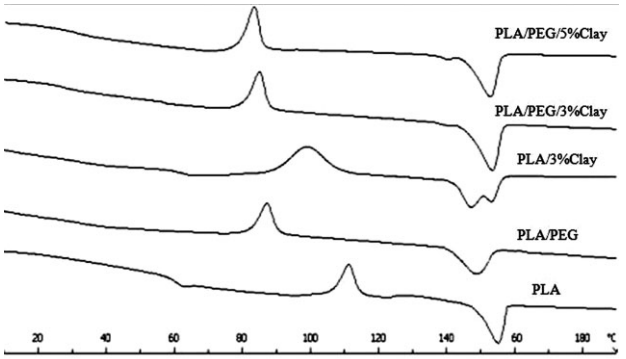

Figure 5 DSC thermograms of PLA, plasticized PLA, and their nanocomposites.

the neat PLA resulted in an increase in T_g. This can be attributed to the restriction of the mobility of the polymer chains as a consequence of bonding or adsorbing on the clay surface. The addition of 20% PEG as a plasticizer to the neat-PLA resulted in $\sim$ 30°C decrease in T_g. This reduction is slightly recovered ($\sim$ 4°C) by the incorporation of clays to the plasticized PLA. Further increase of the clay content does not change the glass transition of the resulting nanocomposite structure.

The addition of plasticizer and/or clay to the PLA affects cold crystallization behavior. The T_c observed in neat PLA at 106.1°C is depressed to 85.1°C with the addition of PEG in the absence of clay. Moreover, the addition of clay also depressed the T_c of the nanocomposite when compared to neat PLA. This indicates that organoclay act as a nucleating agent for PLA crystallization.[17] It was shown by Nam et al. and Ray et al. that the large surface area of the exfoliated clays facilitates the PLA crystallization process. The size of the crystals in PLA nanocomposites was found to be smaller than that of neat-PLA.[5,18] When the plasticizer and the clays are processed together, T_c remained the same for PLA/PEG/3% Clay, whereas it is lowered for PLA/PEG5% Clay nanocomposites in comparison to the PEG/PLA and 3% Clay/PLA systems.

The melting behavior is also influenced by the addition of clay and/or PEG to the PLA. The single melting peak appeared at 152.6°C in neat-PLA is divided into two small peaks (i.e., at 147.2 and 155.3°C) in the case of 3% Clay/PLA nanocomposite indicating the formation of two different crystal types. The addition of PEG to the PLA as the plasticizer lowered ($\sim$ 2°C) the T_m of the resulting blend. Similar observation is also made elsewhere.[19] The plasticization in the presence of clay addition does not change the T_m of the nanocomposites in comparison to neat-PLA. The degree of crystallinity of neat-PLA and plasticized PLA are nearly the same with each other. The addition of clay to these systems enhances the degree of crystallinity about 8%.

Mechanical properties

The results of tensile test are summarized in Table II and the representative stress–strain curves for PLA, PLA/PEG blends, and their nanocomposites are shown in Figure 6. The addition of 3% clay to the neat-PLA does not affect the strength; however, it enhances the modulus of the nanocomposites in comparison to neat-PLA. Furthermore, the addition of clays to the PLA resulted in a decrease in strain at break value. The stress–strain behavior also changed with the addition of clays to the PLA. Neat-PLA exhibits a maximum at the yield point followed by a cold-flow region and finally failure, which is typical for ductile polymers (see Fig. 6). However, in 3% Clay/PLA nanocomposite system, due to the restricted slippage of the polymer chains because of the presence of the clay particles the failure happens just after the yield point without cold flowing. Plasticization of PLA by PEG can be characterized by the significant decrease in strength and modulus and significant increase in strain at break value. The stress–strain behavior of plasticized PLA is characterized by a maximum at yield point and following cold-flow of more than 90% strain before failure. Incorporation of 3% clay to the plasticized PLA improved the modulus with respect to PLA/PEG; on the other hand, the strain at break value is lowered $\sim$ 40%. Further addition of clay (5%) does not change the modulus but lowered the tensile strength and strain at break values. When the stress–strain curves are considered, yielding still exists in the case

TABLE I
Thermal Properties of PLA, Plasticized PLA, and Their Nanocomposites

Material	T_g (°C)	T_c (°C)	T_m (°C)	ΔH_m (J/g)	χ_c (%)
PLA	59.9 ± 0.8	106.1 ± 1.1	152.6 ± 1.1	19.9 ± 2.3	21.4
PLA/PEG	29.4 ± 0.7	85.1 ± 0.7	150.9 ± 0.6	20.5 ± 1.7	22.0
PLA/3% Clay	61.1 ± 0.5	98.9 ± 0.7	147.2 ± 1.1 155.3 ± 1.2	26.7 ± 2.6	28.7
PLA/PEG/3% Clay	33.5 ± 1.1	84.1 ± 0.8	151.6 ± 0.7	28.2 ± 2.3	30.3
PLA/PEG/5% Clay	33.4 ± 0.8	81.6 ± 0.9	152.2 ± 0.8	27.4 ± 1.9	30.5

TABLE II
Summary of the Mechanical Test Results of PLA, PLA/PEG, and Their Nanocomposites

Material	Strength (MPa)	Modulus (MPa)	Strain at break (%)
PLA	33.58 ± 0.8	1406 ± 101	4.91 ± 1.42
PLA/PEG	25.74 ± 0.84	826 ± 28	96.6 ± 8.45
PLA/3% Clay	32.4 ± 1.85	1884 ± 97	2.76 ± 0.62
PLA/PEG/3% Clay	24.95 ± 1.67	1124 ± 74	63.2 ± 12.63
PLA/PEG/5% Clay	20.1 ± 1.5	1130 ± 270	16.2 ± 7.75

of plasticized PLA-based nanocomposites followed by a cold drawing with declining stress.

Biodegradation rate

A major problem of using PLA as a biodegradable material is the slow rate of degradation when compared to other biodegradable materials.[20] The biodegradation of PLA in a composting environment has two steps. In step one, the high-molecular-weight PLA chains hydrolyze to low-molecular-weight oligomers. This step is affected by temperature and moisture. The second step is the conversion of the oligomeric compounds into CO_2, water, and humus by means of microorganisms.[20] Therefore, any factors that increase the hydrolysis tendency can promote the degradation of PLA. Other factors effective in biodegradation of polymers are the molecular weight and the degree of crystallinity.[21] Lower molecular weight chains of PLA may show higher rates of enzymatic degradation because of high concentration of accessible chain end groups.[22] It is known that the amorphous phase is easy to degrade compared with crystal phase. Figure 7 shows the rate of biodegradation of PLA, PLA/PEG, and their nanocomposites. The order of increase in the rate of biodegradation is PLA > PLA/PEG > 3% Clay/PLA/PEG > 5% Clay/PLA/PEG > 3% Clay/PLA. It is clear that the addition of clay retards the rate of biodegradation, although opposite claims are reported in the literature.[20] The 30% of weight loss happens in the first 30 days for PLA, and then the biodegradation rate slows down. For the nanocomposites, the biodegradation is about 10% at the end of 100 days.

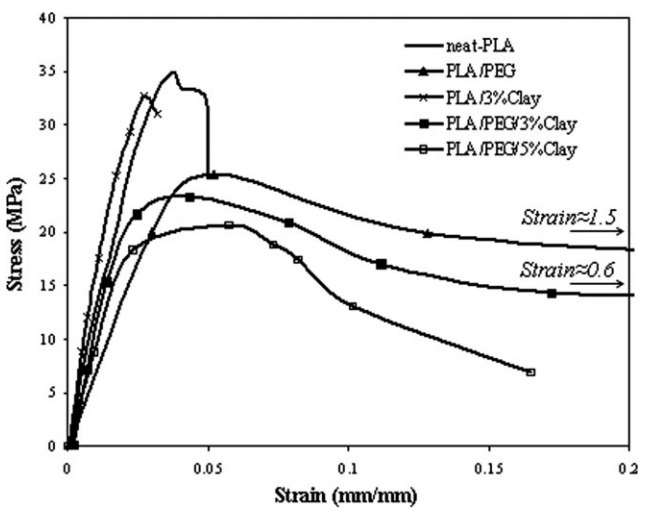

Figure 6 Representative stress–strain curves for PLA, PEG/PLA, and their nanocomposites.

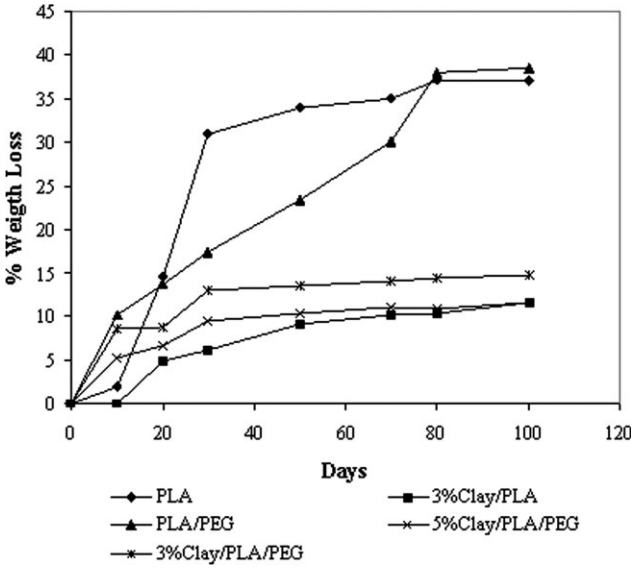

Figure 7 Time dependence of weight loss (%) during biodegradation.

In this study, molecular weight can be assumed to be unchanged because of the same processing history of the materials. Two main factors that can be effective in the biodegradation rates are the difference in hydrophilicity and crystallinity of the films. The hydrophilicities of the films are tested by means of water absorption tests (see Table III). The addition of clay to the PLA increases the water absorption of resulting nanocomposite films, probably due to the hydrophilic character of the Closite 30B. Moreover, plasticization also promotes the water absorption of the films. When the relationship between water absorption and biodegradation rate are considered, a correlation cannot be obtained. Therefore, water

TABLE III
Water Absorptions (%) of PLA, PLA/PEG, and Their Nanocomposites

Materials	Water absorption (%)
PLA	3.1
PLA/PEG	7.7
PLA/3% Clay	6.1
PLA/PEG/3% Clay	14.4
PLA/PEG/5% Clay	14.5

absorption is found to be a nondominant factor in biodegradation. The degree of crystallinity is another factor as mentioned earlier. It is seen that χ_c values get higher by the addition of the clay (see Table II). Therefore, it can be concluded that increasing crystallinity as a result of clay inclusion may be the reason of observing lower rate of biodegradation for the PLA and plasticized PLA-based nanocomposites.

CONCLUSIONS

PLA and PEG-plasticized PLA nanocomposite films including 0, 3, and 5% organoclay are prepared by melt intercalation method using a laboratory scale compounder connected to a cast film device. It is concluded from XRD and TEM results that the exfoliation is predominant in plasticized PLA nanocomposites, whereas the intercalated and unexfoliated agglomerates for the nonplasticized PLA are observed together. Tensile tests indicate that the addition of clay to the neat-PLA does not affect the strength; however, it enhances the modulus of the nanocomposites in comparison to neat-PLA. The incorporation of clay to the plasticized PLA improved the modulus with respect to PLA/PEG. The plasticization effect of PEG is slightly deteriorated by the inclusion of clay. The rate of biodegradation is significantly affected by the incorporation of PEG and/or clay.

The authors are gratefully acknowledged to Mr. Onder Dogan for his experimental assistance in biodegradation tests, DSM Xplore for technical support in the production of films and TEM studies, and Dr. Tamer Sinmazcelik for allowing us to use his laboratory facilities for mechanical tests.

References

1. Pillin, I.; Montrelay, N.; Grohens, Y. Polymer 2006, 47, 4676.
2. Schmidt, D.; Shah, D.; Giannelis, E. P. Curr Opin Solid State Mater Sci 2002, 6, 205.
3. Ray, S. S.; Yamada, K.; Okamoto, M.; Ueda, K. Polymer 2003, 44, 857.
4. Ray, S. S.; Yamada, K.; Okamoto, M.; Ogami, A.; Ueda, K. Chem Mater 2003, 15, 1456.
5. Ray, S. S.; Yamada, K.; Okamoto, M.; Ogami, A.; Ueda, K. Polymer 2003, 44, 6633.
6. Ray, S. S.; Maiti, P.; Okamoto, M.; Yamada, K.; Ueda, K. Macromolecules 2002, 35, 3104.
7. Ray, S. S.; Yamada, K.; Okamoto, M.; Ueda, K. Nano Lett 2002, 2, 1093.
8. Pluta, M.; Galeski, A.; Alexandre, M.; Paul, M. A.; Dubois, P. J Appl Polym Sci 2002, 86, 1497.
9. Martin, O.; Averous, L. Polymer 2001, 42, 6209.
10. Baiardo, M.; Frisoni, G.; Scandola, M.; Rimelen, M.; Lips, D.; Ruffieux, K.; Wintermantel, E. J Appl Polym Sci 2003, 90, 1731.
11. Ljungberg, N.; Wesslen, B. J Appl Polym Sci 2002, 86, 1227.
12. Thellen, C.; Orroth, C.; Froio, D.; Ziegler, D.; Lucciarini, J.; Farrell, R.; Ann D'souza, N.; Ann Ratto, J. Polymer 2005, 46, 11716.
13. Paul, M.-A.; Alexandre, M.; Degee, P.; Henrist, C.; Rulmont, A.; Dubois, P. Polymer 2005, 44, 443.
14. Krikorian, V.; Pochan, D. J. Chem Mater 2003, 15, 4317.
15. Lee, S. Y.; Hana, M. A. Polym Compos, 2009, 30, 665.
16. Migliaresi, C. D.; Cohn, D.; De Lollis, A.; Fambri, L. J Appl Polym Sci 1991, 43, 83.
17. Lewitus, D.; McCarthy, S.; Ophir, A.; Kenig, S. J Polym Environ 2006, 14, 171.
18. Nam, J. Y.; Ray, S. S.; Okamoto, M. Macromolecules 2003, 36, 7126.
19. Pluta, M.; Paul, M. A.; Alexandre, M.; Dubois, P. J Polym Sci Part B: Polym Phys 2006, 44, 299.
20. Ray, S. S.; Okamoto, M. Macromol Rapid Commun 2003, 24, 815.
21. Kawai, F. CRC Crit Rev Biotechnol 1987, 6, 273.
22. Taino, T.; Fukui, T.; Shirakura, Y.; Saito, T.; Tomita, K.; Kaiho, T.; Masamune, S. Eur J Biochem 1982, 124, 71.